

Electronic structure and x-ray magnetic circular dichroism of $\text{Sr}_2\text{FeMoO}_6$: *Ab initio* calculations

V. Kanchana,¹ G. Vaitheeswaran,¹ M. Alouani,^{2,*} and A. Delin¹

¹*Department of Materials Science and Engineering, Royal Institute of Technology, Brinellvägen 23, 10044 Stockholm, Sweden*

²*Institut de Physique et de Chimie des Matériaux de Strasbourg (IPCMS), UMR 7504 CNRS-ULP, 23 rue du Loess, 67034 Strasbourg Cedex, France*

(Received 21 March 2007; revised manuscript received 20 May 2007; published 14 June 2007)

Theoretical investigations of the electronic structure, x-ray absorption, and x-ray magnetic circular dichroism (XMCD) at the Fe $L_{2,3}$ and Mo $L_{2,3}$ edges of $\text{Sr}_2\text{FeMoO}_6$ are carried out by means of the generalized gradient approximation. The magnetic coupling between Fe and Mo is found to be antiparallel, which gives direct confirmation of ferrimagnetic ordering and settles controversies existing between the earlier experimental reports. This is also confirmed by our good agreement of the Mo $L_{2,3}$ edges with experiment. Using our theoretical spectra, we recalculate the spin and orbital magnetic moments by means of the XMCD sum rules and compare the results with a direct self-consistent calculation and experiment.

DOI: [10.1103/PhysRevB.75.220404](https://doi.org/10.1103/PhysRevB.75.220404)

PACS number(s): 71.15.Ap, 71.20.Eh

Soft x-ray magnetic circular dichroism (XMCD), which initially was viewed as quite an exotic technique, has now developed into a standard experimental tool in the exploration of magnetic and electronic properties, with atomic and orbital selectivity. With the help of the sum rules derived by Thole and co-workers,¹ the spin and orbital moments for all inequivalent sites in a crystal can be computed directly from the XMCD spectra. The results from XMCD measurements can be combined in several useful ways with density functional theory. For example, the calculation by Antonov *et al.*² of the XMCD spectra of magnetite Fe_3O_4 , which is a mixed valent material with both Fe^{2+} and Fe^{3+} ions present, showed that Fe atoms occupy two types of sites, tetrahedral ones, called *A*, and octahedral ones, called *B*. All the *A* sites are occupied by Fe^{3+} , whereas at the *B* sites there is a mix of Fe^{2+} and Fe^{3+} . By computing the XMCD spectra from density functional theory, it becomes possible to distinguish between the Fe signals from different sites, aiding the interpretation of the experimental XMCD spectra. Further, Kanchana *et al.*³ have investigated the effect of magnetic anisotropy on XMCD spectra of CrO_2 . They found that the computed XMCD anisotropy is much smaller than the measured one.

$\text{Sr}_2\text{FeMoO}_6$ (SFMO) is a case of special interest due to its technological potential as a spintronics material, and due to the many diverging reports, both theoretical and experimental, on its electronic and magnetic structure. SFMO is a magnetic metal with a gap in one spin channel, i.e., it is a so-called half metal with a Curie temperature T_C of 418 K, exceeding room temperature. The half metallicity causes total spin polarization of the charge carriers. This, in turn, may give rise to a low-field magnetoresistive effect based on intergrain tunneling, which can be explained in a simple model as follows. In a system with a microstructure consisting of half-metallic monodomain grains dispersed in an insulating matrix, the magnetic moments of the magnetic grains are randomly ordered, and the tunneling from grain to grain becomes low, since the moments of two adjacent grains in general are not aligned. As the grain magnetic moments align due to an increasing external magnetic field, the resistance is reduced. Note that there is no need for complete half metallicity, such as that in SFMO, for the magnetoresistive effect to occur. More important is a low coercivity of the material;

otherwise one needs a large magnetic field in order to turn the grain magnetic moments.

The magnetic structure of SFMO single crystals was investigated by two groups^{4,5} using x-ray magnetic circular dichroism at the $L_{2,3}$ edges of Fe and Mo, and contradictory results were obtained regarding the moment induced at the Mo site. Photoemission and x-ray absorption spectroscopic studies on the Mo-based double perovskites concluded a mixed valence state for Fe,⁶ whereas recent neutron diffraction measurements report Fe^{3+} and Mo^{5+} valence states.^{7,8} On the other hand, many other spectroscopic studies also report Fe to be in the +3 state.⁹ The experimentally observed magnetic structure is ferrimagnetic, with large Fe spin moments antiparallel to small Mo spin moments.

In the ionic model, the Fe atoms are in the +3 valence state and the $3d$ shell is exactly half filled, giving a spin moment of $5\mu_B$ and zero orbital moment per Fe atom. The Mo atoms are in the +5 state with one d electron of t_{2g} symmetry in the $4d$ shell. The ionic model implies a charge transfer of one $3d$ and two $4s$ electrons from each Fe atom, and one $5s$ and four $4d$ electrons from each Mo atom. If the remaining Mo d electron were completely localized, it would result in a spin moment of $1\mu_B$ on the Mo site. In the real material the Mo moments are quite small, and one may therefore conclude that the Mo d states are partly delocalized, leading to quenching of both the spin and orbital moments. The half filling of the Fe $3d$ shell leads to an interesting effect. Since it is half filled, only electrons of opposite spin can hop into the Fe d shell due to the Pauli principle. This means that we must have an antiferromagnetic coupling between the Fe and Mo d states, leading to a ferrimagnetic ground state. In energy terms, the kinetic energy in SFMO is thus minimized when the local Fe moments are parallel to each other and antiparallel to the itinerant Mo spins, resulting in the observed ferrimagnetic structure.¹⁰

In the present work, we have calculated the electronic properties and the x-ray absorption (XAS) and XMCD spectra at the Fe $L_{2,3}$ and Mo $L_{2,3}$ edges of SFMO. Using our theoretical spectra, we recalculate the spin and orbital magnetic moments and compare them to the moments resulting from a direct self-consistent calculation. The comparison with experiment allows us to understand the magnetic cou-

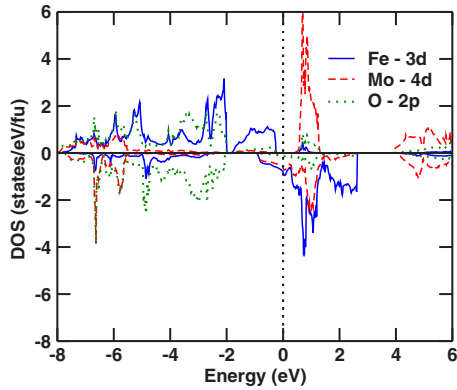


FIG. 1. (Color online) Calculated spin-resolved partial density of states (DOS) of SFMO per formula unit (f.u.). The DOS of $3d$ Fe is blue (continuous line), that of $4d$ Mo red (dashed line), and that of $2p$ O green (dotted line). The majority and minority spins are shown, respectively, in the positive and negative DOS scales.

pling between the Fe and Mo sites and the ferrimagnetic ground state of SFMO. In particular, we have found that the Fe and Mo spin moments are aligned antiparallel, in agreement with the experimental results.

The present density functional theory calculations were performed using an all-electron full-potential linear muffin-tin orbital method (FPLMTO) including the spin-orbit coupling (SOC), which has been described in detail elsewhere.¹¹ We expanded the spherical harmonics up to $l_{max}=6$ and used a double basis so that each orbital is described using two different kinetic energies in the interstitial region. Furthermore, we included several pseudocore orbitals in order to further increase accuracy. Thus, the valence-electron basis set consisted of the Sr ($4s5s4p5p4d$), Fe ($4s3p4p3d$), Mo ($5s4p5p4d$), and O ($2s2p$) LMTOs. The implementation of the XMCD calculations has been described elsewhere¹² and it is similar to that of Wu *et al.*¹³

We performed our calculations using the experimental structure and atomic positions, i.e., the tetragonal structure with space group symmetry $I4/m$, with the experimental cell parameters⁸ $a=b=5.55$ Å and $c=7.90$ Å. The radii of the muffin-tin spheres used for Sr, Fe, Mo, and O were 1.32, 1.1, 1.0, and 0.85 Å, respectively. The direction of the spin magnetic moment was chosen to be along the c axis. The integration in reciprocal space was performed using 210 \mathbf{k} points in the irreducible Brillouin zone (BZ), corresponding to 1458 \mathbf{k} points in the full BZ for our self-consistent ground-state calculation. We used the generalized gradient approximation¹⁴ to the exchange-correlation functional.

Our calculated partial density of states (DOS), shown in Fig. 1, agrees well with earlier calculations.^{15–18} The (nearly) cubic symmetry of the octahedral coordination of the oxygen atoms around the transition metals splits, in a simplified picture, the d levels into one peak of t_{2g} states, and another peak of e_g states, with the t_{2g} states having the lower energy. The main feature in the DOS is a gap between the Fe e_g states and Mo t_{2g} states in one of the spin channels, causing the half-metallic electronic structure. From our ground-state calculation, we find 0.2 $4s$ and 4.6 $3d$ electrons within the Fe muffin-tin sphere, and 0.1 $5s$ and 2.2 $4d$ electrons within the

TABLE I. Spin and orbital d magnetic moments in μ_B /atom for $\text{Sr}_2\text{FeMoO}_6$ obtained from the self-consistent (SC) calculation and from the sum rules (SR), along with the experimental XMCD values taken from Ref. 5.

	Spin			Orbital		
	SC	SR	Expt.	SC	SR	Expt.
Fe	3.72	3.84	3.05 ± 0.2	0.042	0.055	0.02 ± 0.02
Mo	-0.29	-0.29	-0.32 ± 0.05	0.020	0.056	-0.05 ± 0.05

Mo sphere. It is the inevitable nature of chemical compounds that the concept of valence of individual atoms becomes vague, a situation also reflected in results from electronic structure calculations. Thus, one cannot derive a unique valence state using exclusively the occupation numbers above. However, we can safely conclude that the relative d electron transfer from the Fe and Mo atoms appears to be exaggerated in the standard ionic model used for SFMO, and that the d electrons at both the Fe and Mo sites should be regarded as at least partly delocalized.

By comparing the spin-resolved partial DOS in Fig. 1 with a calculation where the SOC is excluded,¹⁷ we find that the SO coupling induces a small splitting of the Fe t_{2g} and Mo t_{2g} states. SFMO remains half metallic with the SOC included, which is in contrast to the Re-based double perovskites, where the inclusion of SOC eventually destroys the band gap, resulting in a pseudo-half-metallic ground state.¹⁹ A possible reason could be that the SOC parameter of Mo is slightly smaller when compared to that of the $5d$ transition metal Re. In addition to that, the half-metallic gap in SFMO is significantly larger than that of the Re compounds, which helps in preserving the half-metallic ground state.

The total spin moment per unit cell is found to be $4\mu_B$, in agreement with previous calculations. Notice that, even though 14.72 electrons are present in the whole interstitial region per formula unit, their spin polarization is negligible. The Fe spin and orbital moments are parallel, whereas the spin and orbital Mo moments are antiparallel, in accordance with Hund's third rule. In Table I, we have listed our calculated magnetic moments. Our calculated spin magnetic moment of $3.72\mu_B$ for Fe is 2% lower than in earlier calculations ($3.79\mu_B$ – $3.8\mu_B$).^{16–18} The orbital Fe magnetic moment of $0.042\mu_B$ is very close to the FPLMTO result of Jeng and Guo¹⁸ ($0.043\mu_B$). The calculated spin moment of the Mo atom, $-0.29\mu_B$, is the same as the one obtained in earlier calculations [$0.29\mu_B$ – $0.3\mu_B$ (Refs. 16–18)]. We find an orbital moment of $0.020\mu_B$ at the Mo site, whereas Jeng and Guo's¹⁸ value is $0.032\mu_B$. The relative difference between these two values is large, but in absolute values, the difference is $0.012\mu_B$ which is the level of precision to be expected from electronic structure calculations. The results from different calculations may vary somewhat since the calculated moments depend on the details of the calculations and especially on the sizes of the muffin-tin spheres. Finally, our calculations give an induced spin moment on the oxygen atom of about $0.09\mu_B$, which is comparable to that ($0.5\mu_B$ for six oxygens) reported from earlier calculations¹⁶ but is

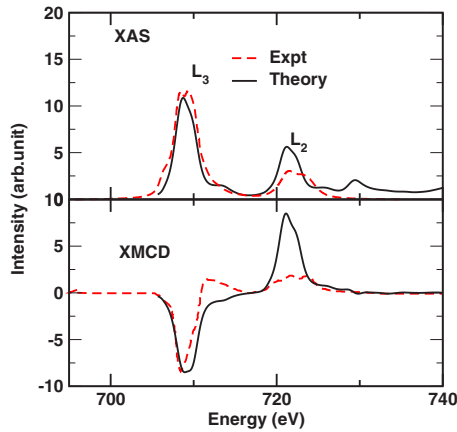


FIG. 2. (Color online) Calculated XAS and XMCD spectra of Fe $L_{2,3}$ edges (full lines) as compared to the experimental data of Ref. 5 (dashed lines).

significantly larger than the experimental XMCD estimate in Ref. 5.

Comparing with experimental data, our calculated Fe spin moment is, just as earlier calculations, between the experimental XMCD result⁵ ($3.05\mu_B$) and the neutron diffraction value⁸ ($3.91\mu_B$). In contrast, our calculated Mo spin moment is 9–22 % smaller than the experimental results from both XMCD (Ref. 5) ($-0.32\mu_B$) and neutron diffraction⁸ ($-0.37\mu_B$) experiments. Notice that the experimental neutron diffraction data add up to a saturation moment close to the ideal value of $4\mu_B$ or measured value $3.9\mu_B$,⁸ if we assume a total spin moment of about $0.5\mu_B$ for the six oxygens,^{8,18} whereas the XMCD produced a far lower saturation value. The lower reported spin moments in the XMCD experiment compared to neutron diffraction may be due to Fe-Mo antisite disorder of the sample, estimated to be between 10% and 15%.^{5,20} Regarding the orbital moments, both Fe and Mo values are very small (a few hundredths of a μ_B), consistent with the XMCD experiments.⁵

Figures 2 and 3 show the calculated x-ray absorption and XMCD spectra of the Fe $L_{2,3}$ and Mo $L_{2,3}$ edges. We convoluted our spectra using a Lorentzian followed by a Gaussian, both of full width at half maximum (FWHM) of 0.25 eV for

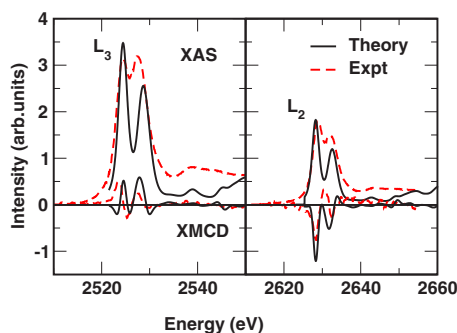


FIG. 3. (Color online) Calculated XAS and XMCD spectra of Mo L_2 and L_3 edges (full lines) as compared to the experimental results of Ref. 5 (dashed lines). We have used a FWHM of 0.5 eV to broaden the spectra.

Fe and 0.5 eV for Mo. The Gaussian and Lorentzian broadenings represent, respectively, the experimental resolution and the width of the core hole. The calculated spin-orbit splitting of the Fe $2p$ core states is 12.52 eV, in good agreement with the experimental separation between the L_2 and L_3 edges of 12.5 eV.⁵ The corresponding splitting for Mo is 106.5 eV.

The upper panel of Fig. 2 shows the XAS of the Fe $L_{2,3}$ edges and the lower panel the XMCD spectra together with the experimental spectra of Besse *et al.*⁵ The calculations reproduce most features of the experimental spectra, but at the qualitative level. We find that the L_2 intensity is overestimated in the absorption spectra. The same situation prevails in many other compounds³ and can be improved by taking into account the core-hole interaction.¹² Interestingly, at both Fe absorption edges in the experimental spectra of Besse *et al.*⁵ there is a slight doublet structure present, interpreted by Besse *et al.* as signaling the presence of both Fe^{2+} (d^6) and Fe^{3+} (d^5) in SFMO. In the XMCD spectra by Ray *et al.*,⁴ however, a corresponding doublet structure is not visible. We speculate that the doublet structure is sensitive to the exact composition of the sample, e.g., the amount of antisite disorder and/or oxygen and other vacancies and not primarily connected to the intrinsic electronic structure of ideal SFMO. This conclusion is supported by the self-interaction-corrected calculations by Szotek *et al.*,²¹ which basically rule out the possibility of any Fe^{2+} valence in SFMO. They find that the Fe^{3+} valence is the most energetically favorable one, with Fe^{4+} 0.83 eV more unstable and Fe^{2+} 1.66 eV more unstable than the Fe^{3+} valence. Further support is provided by our calculated d occupation numbers—4.6 Fe $3d$ electrons is entirely consistent with a total of five electrons in the Fe $3d$ shell.

Our Fe XMCD spectrum shown in the lower panel of Fig. 2 reveals a sharp signal indicating a large value of the Fe moment. Using the XMCD sum rules (see below), we find a Fe spin magnetic moment of $3.84\mu_B$, which is 3% higher than our direct calculation, but still between the experimental values derived from XMCD and neutron diffraction experiments. As for the very small ($0.055\mu_B$) Fe orbital moment recalculated from the spectra in the same way, we find that it, just like the spin moment, is larger compared to the direct calculation.

The calculated XAS and XMCD spectra of the Mo $L_{2,3}$ edges are shown in Fig. 3, and are in surprisingly good agreement with those of Besse *et al.*,⁵ especially considering that the Mo moments are nearly quenched in this system. Although the Mo $5d$ states are rather delocalized, an appreciable electron density is still present at the Mo site which results in a pronounced XMCD signal, evident in Fig. 3. The spin moment for Mo obtained from the XMCD sum rule is identical to the value from the direct calculation. As for the orbital moment of Mo, the sum rule produces a significantly higher value compared to the direct calculation. Thus, the serious controversy regarding the existence of an XMCD signal at the Mo site (see Ref. 5) or not (see Ref. 4) has been solved by our theoretical calculation.

It is important to mention that the spin and orbital XMCD sum rules are derived using many approximations.¹ The most

important ones are that the radial matrix elements are assumed to be energy independent, and differences in the radial wave functions are ignored. In some cases the approximations can actually give rise to quite large errors.²² Here we used Eqs. (6) and (7) of Carra *et al.*¹ to calculate, respectively, the orbital and spin moments. We have neglected the expectation value of the magnetic dipole term, which is usually very small. To extract both the spin and orbital moments we need to calculate the number of holes and the energy cutoff for the integration of the XMCD spectra. Because 14.72 unpolarized electrons are in the interstitial region, the number of d holes has to be determined by integrating the unoccupied atom-resolved d DOS up to the energy cutoff, and not by subtraction the valence d electrons from ten states. We found that an energy cutoff of 10 eV produced the total d hole count of 4.2 for Fe, and 6.3 for Mo. Notice that the XMCD, through the sum rules, determines only the part of the magnetic moments in the atomic region where the core wave function (here the $2p$ state) is localized. The Fermi golden rule matrix elements are therefore calculated only in the muffin-tin region. This might be one of the reasons why the XMCD magnetic moments are smaller than the ones obtained using neutron diffraction experiments.

In conclusion, we have used the FPLMTO method to calculate the ground-state electronic structure, the XAS, and the XMCD at both the Fe $L_{2,3}$ and Mo $L_{2,3}$ edges. Comparing our results to existing experimental and theoretical results we find a semiquantitative agreement with experimental XAS and the XMCD spectra. The pronounced signal at the Mo $L_{2,3}$ edge clearly solves the experimental controversies regarding the existence of a spin moment at the Mo site and establishes the ferrimagnetic nature of this compound. Our data also support the view that the d states at the Fe and Mo sites are partly delocalized. The sum-rule-computed spin moments are in very good agreement with both values obtained from direct calculation and experiments. The calculated orbital moments are all very small—on the level of a few hundredths of a μ_B —and the sum-rule-computed values are larger than the directly computed ones. The differences between our calculated orbital moments, other calculations, and experiment are on the level of the precision of the experimental values.

V.K., G.V., and A.D. acknowledge financial support from VR and SSF, and M.A. the ANR Grant No. 06-NANO-053-01. SNIC is acknowledged for providing computer time.

*mea@ipcms.u-strasbg.fr

- ¹B. T. Thole, P. Carra, F. Sette, and G. van der Laan, *Phys. Rev. Lett.* **68**, 1943 (1992); P. Carra, B. T. Thole, M. Altarelli, and X. Wang, *ibid.* **70**, 694 (1993).
- ²V. N. Antonov, B. N. Harmon, and A. N. Yaresko, *Phys. Rev. B* **67**, 024417 (2003).
- ³V. Kanchana, G. Vaitheeswaran, and M. Alouani, *J. Phys.: Condens. Matter* **18**, 5155 (2006).
- ⁴S. Ray, A. Kumar, D. D. Sarma, R. Cimino, S. Turchini, S. Zennaro, and N. Zema, *Phys. Rev. Lett.* **87**, 097204 (2001).
- ⁵M. Besse, V. Cros, A. Barthélémy, H. Jaffrès, J. Vogel, F. Petroff, A. Mirone, A. Tagliaferri, P. Bencok, P. Berthet, Z. Szotek, W. M. Temmerman, S. S. Dhesi, N. B. Brookes, A. Rogalev, and A. Fert, *Europhys. Lett.* **60**, 608 (2002).
- ⁶J.-S. Kang, J. H. Kim, A. Sekiyama, S. Kasai, S. Suga, S. W. Han, K. H. Kim, T. Muro, Y. Saitoh, C. Hwang, C. G. Olson, B. J. Park, B. W. Lee, J. H. Shim, J. H. Park, and B. I. Min, *Phys. Rev. B* **66**, 113105 (2002).
- ⁷Y. Moritomo, S. Xu, A. Machida, T. Akimoto, E. Nishibori, M. Takata, M. Sakata, and K. Ohoyama, *J. Phys. Soc. Jpn.* **69**, 1723 (2000).
- ⁸D. Sánchez, J. A. Alonso, M. García-Hernández, M. J. Martínez-Lope, J. L. Martínez, and A. Mellergård, *Phys. Rev. B* **65**, 104426 (2002); D. Sánchez, J. A. Alonso, M. García-Hernández, M. J. Martínez-Lope, and M. T. Casais, *J. Phys.: Condens. Matter* **17**, 3673 (2005).
- ⁹M. S. Moreno *et al.*, *Solid State Commun.* **120**, 161 (2001); K. Kuepper *et al.*, *Phys. Status Solidi A* **15**, 3252 (2004); J. Herrero-Martín, J. García, G. Subías, J. Blasco, and M. C. Sánchez, *Phys. Scr.*, T **115**, 471 (2005).
- ¹⁰G. Jackeli, *Phys. Rev. B* **68**, 092401 (2003).
- ¹¹J. M. Wills, O. Eriksson, M. Alouani, and D. L. Price, in *Electronic Structure and Physical Properties, of Solids*, edited by H. Dreyssé (Springer, Berlin, 2000).
- ¹²M. Alouani, J. M. Wills, and J. W. Wilkins, *Phys. Rev. B* **57**, 9502 (1998).
- ¹³R. Wu, D. Wang, and A. J. Freeman, *Phys. Rev. Lett.* **71**, 3581 (1993).
- ¹⁴J. P. Perdew, K. Burke, and M. Ernzerhof, *Phys. Rev. Lett.* **77**, 3865 (1996).
- ¹⁵D. D. Sarma, P. Mahadevan, T. Saha-Dasgupta, S. Ray, and A. Kumar, *Phys. Rev. Lett.* **85**, 2549 (2000).
- ¹⁶T. Saha-Dasgupta and D. D. Sarma, *Phys. Rev. B* **64**, 064408 (2001).
- ¹⁷K. I. Kobayashi, T. Kimura, H. Sawada, K. Terakura, and Y. Tokura, *Nature (London)* **395**, 677 (1998).
- ¹⁸H. T. Jeng and G. Y. Guo, *Phys. Rev. B* **67**, 094438 (2003).
- ¹⁹G. Vaitheeswaran, V. Kanchana, and A. Delin, *Appl. Phys. Lett.* **86**, 032513 (2005).
- ²⁰A. S. Ogale *et al.*, *Appl. Phys. Lett.* **75**, 537 (1999).
- ²¹Z. Szotek, W. M. Temmerman, A. Svane, L. Petit, and H. Winter, *Phys. Rev. B* **68**, 104411 (2003).
- ²²R. Wu and A. J. Freeman, *Phys. Rev. Lett.* **73**, 1994 (1994).